Polymer 304 (2024) 127149

Contents lists available at ScienceDirect

Polymer

journal homepage: www.elsevier.com/locate/polymer

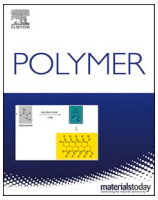

Amphiphilic polymer Co-networks based on cross-linked tetra-PEG-*b*-PCL star block copolymers

Carolin Bunk [a,b], Nora Fribiczer [c], Löser Lucas [d], Martin Geisler [a], Voit Brigitte [a,b], Sebastian Seiffert [c], Kay Saalwächter [d], Michael Lang [a,**], Frank Böhme [a,*]

[a] Leibniz-Institut für Polymerforschung Dresden e. V, Hohe Str. 6, 01069, Dresden, Germany
[b] Organic Chemistry of Polymers, Technische Universität Dresden, 01062, Dresden, Germany
[c] Department of Chemistry, Johannes Gutenberg University Mainz, Duesbergweg 10-14, 55128, Mainz, Germany
[d] Institut für Physik - NMR, Martin-Luther-Universität Halle-Wittenberg, Betty-Heimann-Str. 7, 06120, Halle, Germany

ARTICLE INFO

Keywords:
Amphiphilic polymer co-networks
Amphiphilic star block copolymers
Hetero-complementary coupling reactions
Multiple quantum NMR
Swelling
Rheology

ABSTRACT

A new class of AB_4-type amphiphilic polymer co-networks (ACN) was prepared by hetero-complementary 2-(4-nitrophenyl)-benzoxazinone/amine end group cross-linking chemistry in dimethyl sulfoxide (DMSO). For this purpose, a well-defined star block copolymer (tetra-PEG-*b*-PCL) consisting of a hydrophilic tetra-arm PEG core ($M_n \sim 5$ kg mol^{-1}) and hydrophobic PCL wings with a total molar mass of $M_n \sim 10$ kg mol^{-1} was synthesized by ring-opening polymerization (ROP). This tetra-PEG-*b*-PCL star block copolymer was functionalized either with 2-(4-nitrophenyl)-benzoxazinone or with amino terminal groups. The ACN synthesis was carried out by conversion of these two star block copolymers. The overlap concentration of $c^* \sim 76$ g L^{-1} determined by viscosity measurements of both stars showed no significant temperature dependence. The network syntheses carried out at different concentrations (0.5 c^* to 2.5 c^*) resulted in conversion degrees in the range of $p \approx 95$ % or higher as detected by HR MAS NMR spectroscopy. As in previous work on the synthesis of A_4B_4 networks using the same cross-linking chemistry, deviations from the expected network structure (increased proportion of double links between two stars) were detected also here by multi quantum NMR spectroscopy. The expected environmentally sensitive behavior of the ACNs was confirmed in terms of their equilibrium swelling in solvents of different quality to PEG and PCL. The scaling of the swelling and viscoelasticity data as a function of preparation concentration showed deviations from the expectations of a perfectly cross-linked star polymer network. Finally, a two-step gelation process was observed by rheology at 30 °C in DMSO, which is related to associations between the 2-(4-nitrophenyl)-benzoxazinone groups surrounded by PCL blocks that become apparent on the time scale of rheology when the molar mass is increased as a result of cross-linking.

1. Introduction

Amphiphilic polymer co-networks (ACNs) and gels provide elastic matrices that allow for a co-continuous transport of hydrophilic and hydrophobic solutes depending on the thermodynamic state of the sample [1,2]. When exposed to a selective solvent of a particular philicity, the poorly soluble polymer separates on the nanoscale forming irregular domains that depend on the local composition of both polymer components and the structure of the network. For block copolymer melts and solutions, it is well established that regular patterns can be designed by a suitable choice of the polymer blocks, the polymer architecture, and the solvent [3–5]. These patterns can be guided into a particular direction, for instance, by shearing the polymer domains [6,7]. Similarly, in networks made of different components, a long-range orientational order can be imposed by sample deformation [8]. When applied to amphiphilic gels or networks made from different polymer blocks, these concepts can be used to design new materials with oriented domains that can be prepared or switched on demand [9] leading eventually to a controllable transport of different classes of solutes in different directions. However, for a basic understanding of these processes, model samples are needed that allow a separate control of the key material parameters.

* Corresponding author.
** Corresponding author.
E-mail address: Boehme@ipfdd.de (F. Böhme).

https://doi.org/10.1016/j.polymer.2024.127149
Received 11 January 2024; Received in revised form 30 April 2024; Accepted 6 May 2024
Available online 9 May 2024

In recent years, we have developed a platform of such model networks based upon the hetero-complementary coupling reaction [10–12] of amine- and 2-(4-nitrophenyl)-benzoxazinone-terminated network components. The hetero-complementary strategy has the advantage of avoiding network defects like pending loops that become abundant in the vicinity of the overlap concentration [13,14]. In consequence, model networks can be prepared with a low variation in the connectivity of the branching units over a broad range of concentrations [15,16], which is highly favorable for a concise test of basic physical concepts. In the synthesis of ACNs based on hydrophilic tetra-PEG and hydrophobic tetra-PCL stars, this 2-(4-nitrophenyl)-benzoxazinone/amine reaction has been well established [10,15,17–19]. Nevertheless, it should be noted that the linkage of purely hydrophilic and hydrophobic components as described in Ref. [10] may be accompanied by separation processes that can strongly affect the course of the reaction and the final structure of the network. This is especially important if the solvent used in the synthesis provides a different solvent quality for the two components. In order to better understand the structure-forming processes, star block copolymers are used in this work in which both components are already included. Specifically, these are two batches of tetra-arm star block copolymers consisting each of a PEG core and PCL wings differing only in their end-groups (2-(4-nitrophenyl)- benzoxazinone and amine, respectively). Apart from the end groups, the structural parameters of both stars are equal. Therefore, their solubilities should hardly differ.

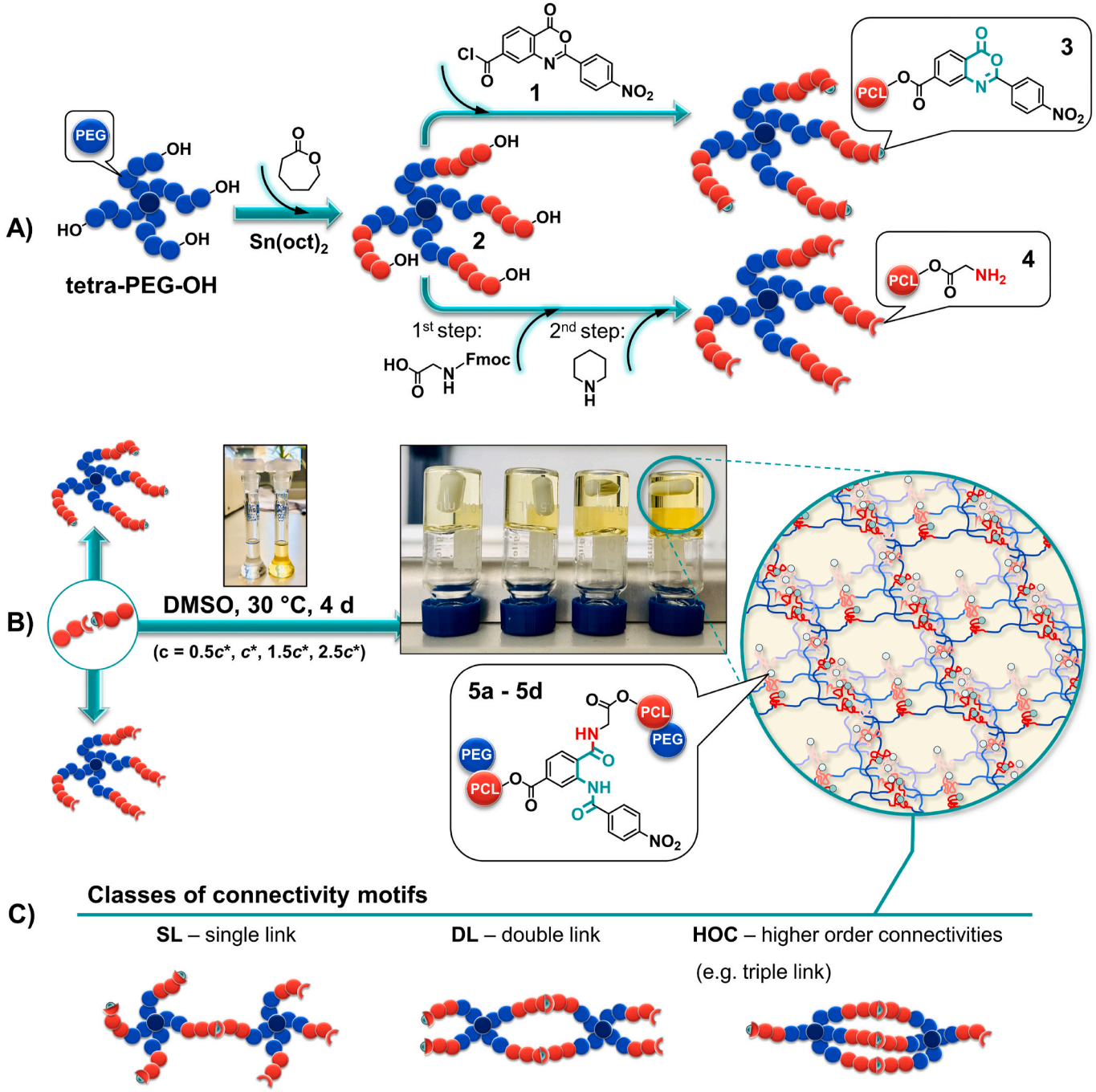

Scheme 1. A) Synthesis of hydroxy-terminated tetra-PEG-*b*-PCL star block copolymer **2**, 2-(4-nitrophenyl)-benzoxazinone-terminated tetra-PEG-*b*-PCL star block copolymer **3**, amino-terminated tetra-PEG-*b*-PCL star block copolymer **4**, and their hetero-complementary reaction B) to obtain amphiphilic polymer co-networks **5a - 5d** with different classes of possible connectivity motifs C).

The synthesis of the star block copolymers, the corresponding ACN formation in dimethyl sulfoxide (DMSO), and their possible connectivity motifs between the same pair of stars are illustrated in Scheme 1.

Combining different blocks in a star polymer provides several additional features that can be utilized to optimize the synthesis or to design a particular morphology of the copolymer networks. First, since all reactive groups are attached to the same polymer block, it is no more mandatory to use a co-solvent for both blocks. Instead, the reactive groups can be concentrated inside nano-domains by choosing a good selective solvent for the star cores. Depending on interactions and temperature, this may create already a reversible or irreversible gel similar to linear ABA block copolymers [20–22] prior to the percolation of the covalent bonds. On the contrary, the star cores can be assembled into nano-domains exposing the reactive groups to a good selective solvent for the outer blocks of the arms [23,24]. In both cases, the concentration of the polymers and the molar masses of the polymer blocks dictate which block copolymer morphology will be selected prior or during the cross-linking of the gel [25]. Introducing order by phase separation prior to cross-linking like in Refs [[26–28]]. may allow to suppress the random perturbation of morphology by the elasticity of the network. This is advantageous for obtaining order on longer range than previously [29], where only ellipsoidal domains with a quickly decaying order were obtained. For anisotropic domains (cylinders and lamella), this provides the opportunity to tailor an anisotropic deformation behavior or local anisotropic transport properties of the materials beyond controlling overlap and spatial orientation of the star polymer through the assembly process. The star polymers of the present study open this playground for the current series of amphiphilic star polymer model networks.

In this study, we will focus more on chemical aspects. Since linear block copolymers with a similar molar mass as our block-stars are soluble in DMSO [30], one goal of this work is to test whether or not DMSO allows to suppress associations between the linking groups during cross-linking that perturbed an experimental analysis of the different network connectivities (see Scheme 1c) in preceding work [10]. Morphological investigations play a secondary role here and are reserved for future investigations. We expect that our results impact further development of switchable amphiphilic model systems with a controlled transport of solutes of different philicity.

2. Experimental section

2.1. Materials

Hydroxy-terminated poly (ethylene glycol) star polymer (**tetra-PEG-OH**) was purchased from JenKem Technology, USA. Prior to use, **tetra-PEG-OH** was first dialyzed against water (ZelluTrans, Roth, dialysis membrane *MWCO* 1000) and subsequently precipitated twice from THF in cold diethyl ether. The number-average molar mass (M_n) and the dispersity ($Đ$) were determined via MALDI-TOF MS ($M_n = 5.2$ kg mol^{-1}, $Đ = 1.01$). The number-average degree of polymerization (P_n) of 116 was determined by ^{1}H NMR spectroscopy, corresponding to an M_n of 5.2 kg mol^{-1}. ε-Caprolactone (ε-CL, 97 %, Sigma-Aldrich) was dried with calcium hydride (CaH_2) for 24 h, then distilled under vacuum and stored under nitrogen atmosphere. Stannous octoate ($Sn(oct)_2$, 98.0 %, Sigma-Aldrich) was purified by vacuum distillation and kept under nitrogen atmosphere. *N*-alpha-(9-fluorenylmethyloxycarbonyl)-glycine (**Fmoc-Gly-OH**, ≥99.0 %) was obtained from Merck KGaA (Novabiochem®), Germany, and used as supplied. Deuterated dimethyl sulfoxide (DMSO-d_6, 99.80 % D, Eurisotop, Germany), dimethyl sulfoxide (DMSO, 99.9 %, Acros Organics), *tert*-butyl methyl ether (MTBE, 99 %, Alfa Aesar), tetrahydrofuran (THF, 99.6 %, Acros Organics), *N*,*N*-dimethylformamide (DMF, (≥99.8 %, VWR chemicals) chloroform (≥99.8 %, Fisher Chemicals), diethyl ether (≥99.5 %, stabilized, Th. Geyer (CHEMSOLUTE®)), piperidine (≥99.0 %, Iris Biotech GmbH), *N*,*N*′-dicyclohexylcarbodiimide (DCC, >97.0 %, TCI chemicals), triethylamine (≥99.5 %, Sigma-Aldrich), and 4-dimethylaminopyridine (DMAP, ≥99.8 %, Sigma-Aldrich) were used without further purification. The synthesis of 2-(4-nitrophenyl)-4-oxo-4H-benzo[d][1,3]oxazine-7-carboxylic acid chloride (**1**) has been described earlier [11].

2.2. Synthesis and functionalization of tetra-PEG-b-PCL star block copolymers

*Hydroxy-terminated tetra-PEG-b-PCL star block copolymer (**2**).* To obtain star block copolymer **2**, ring-opening polymerization (ROP) of ε-CL initiated by **tetra-PEG-OH** with $Sn(oct)_2$ as catalyst was performed according to our previous publications (see Scheme 1A) [10,11]. A typical ROP, **tetra-PEG-OH** (1 eq., 30 g, 5.77 mmol) with a number-average molar mass of 5.2 kg mol^{-1} was dissolved in 31.2 mL ε-CL (46 eq., 30.3 g, 0.265 mol) for 20 min at 80 °C. Subsequently, the polymerization was started by adding $Sn(oct)_2$ (0.05 eq., 0.57 mL of 0.5 M solution in toluene) under a continuous flow of nitrogen. After stirring for 2 h at 80 °C, the temperature was increased to 100 °C for another 3.5 h. The polymerization was stopped by cooling to room temperature and the product was then isolated by precipitation in cold diethyl ether. After washing the product vigorously with fresh diethyl ether, filtering through a filter funnel, and drying *in vacuo* at 40 °C overnight, tetra-PEG_{116}-*b*-PCL_{44} star block copolymer **2** was obtained as a white powder. Yield: 58 g (96 %).

^{1}H NMR (DMSO-d_6): δ 4.30 (t, 5.1 Hz; 11), 4.11 (t, 4.7 Hz; 4*), 3.98 (t, 6.4 Hz; 10), 3.51 (s; 3, 4), 3.40–3.34 (m; 10*), 3.29 (s; 2), 2.27 (t, 7.1 Hz; 6), 1.60–1.45 (m; 7, 9), 1.30 ppm (m; 8). The determination of the block ratio by ^{1}H NMR spectroscopy, the corresponding chemical structures, and the proton signal assignments are reported in the SI (Figs. S1 and S2b).

*2-(4-Nitrophenyl)-benzoxazinone-terminated tetra-PEG-b-PCL star block copolymer (**3**).* Star block copolymer **3** was synthesized by attaching 2-(4-nitrophenyl)-4-oxo-4H-benzo[d][1,3]oxazine-7-carboxylic acid chloride (**1**) (8 eq., 5.13 g, 15.54 mmol) to the hydroxyl terminal groups of star block copolymer **2** (1 eq., 20 g, 1.94 mmol) in the presence of triethylamine (8 eq., 1.57 g, 15.54 mmol) (Scheme 1A). Yield: 19 g (85 %). Details of the reaction are reported elsewhere [10–12].

^{1}H NMR (DMSO-d_6): δ 8.50–8.39 (m; 21, 22), 8.32 (d, 8.1 Hz; 13), 8.20 (s; 16), 8.15 (d, 8.1 Hz; 12), 4.35 (t, 6.1 Hz; 10*), 4.11 (m; 4*), 3.98 (m; 10), 3.51 (s; 3, 4), 3.29 (s; 2), 2.26 (m; 6), 1.53 (m; 7, 9), 1.29 ppm (m; 8). The corresponding chemical structures and the proton signal assignments are given in the SI (Fig. S2c).

*Amino-terminated tetra-PEG-b-PCL star block copolymer (**4**).* Star block copolymer **4** was synthesized according to Scheme 2A in two steps. First, the hydroxyl terminal groups of star block copolymer **2** were esterified with *N*-alpha-(9-fluorenylmethyloxycarbonyl)-glycine (**Fmoc-Gly-OH**) by the Steglich method [31,32], after which the α-amino group was deprotected by piperidine. A representative experiment is described as follows: Star block copolymer **2** (1 eq., 30.0 g, 2.91 mmol) was dissolved in 150 mL of a mixture of DCM and DMF (2:1). After cooling the solution to 0 °C, **Fmoc-Gly-OH** (8 eq., 6.9 g, 23.30 mmol) and DMAP (0.4 eq., 142.2 mg, 1.16 mmol) were added and the mixture was stirred at 0 °C under nitrogen for 30 min. To activate the carboxyl group of **Fmoc-Gly-OH**, 40 mL of a previously prepared solution of DCC (7 eq., 4.2 g, 20.37 mmol) in DCM and DMF (as above 2:1) was added dropwise under nitrogen. The mixture was stirred at 0 °C for 1 h and at room temperature for another 23 h. Then, precipitated dicyclohexylurea was removed by filtration first at room temperature and then at −20 °C. Subsequently, the filtrate was concentrated *in vacuo* and precipitated in cold diethyl ether. After washing the product with fresh diethyl ether, filtering, and drying *in vacuo* at 35 °C overnight, the precipitation was performed one more time. The corresponding chemical structure and the proton signal assignments of the intermediate Fmoc-glycine-terminated tetra-PEG-*b*-PCL star block copolymer are given in the SI (Fig. S3b). To deprotect the α-amino group, the intermediate was dissolved in 100 mL

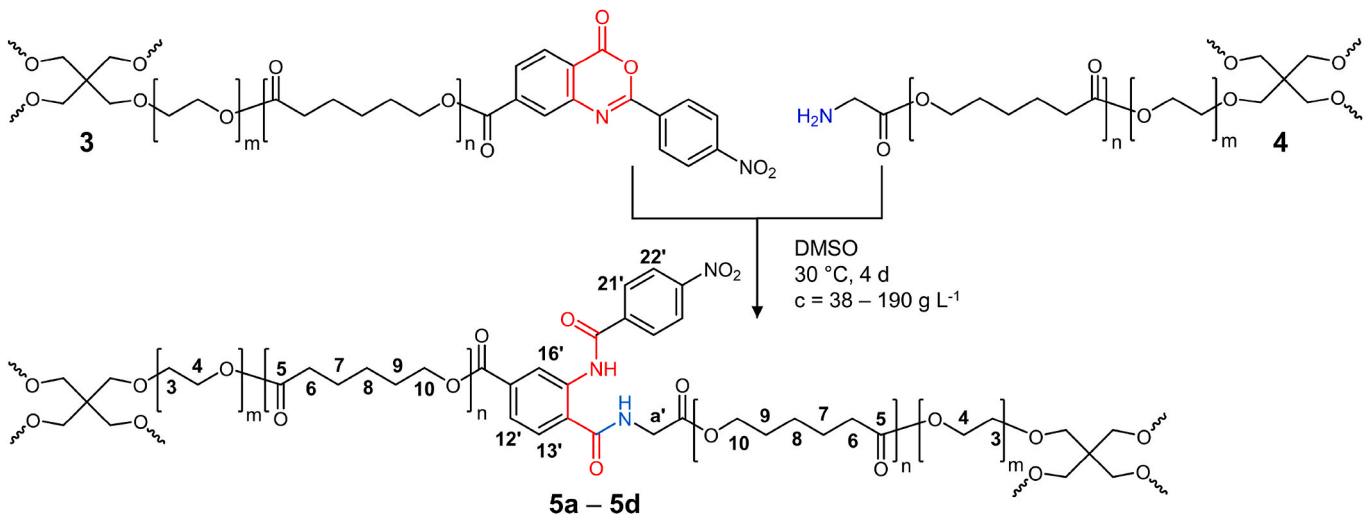

Scheme 2. Synthesis of amphiphilic polymer co-networks (**5a** – **5d**).

of a piperidine/DMF mixture (20 % v/v). The mixture was stirred at room temperature for 1 h, filtered off, and the filtrate was precipitated in cold n-hexane. n-Hexane was decanted, and the waxy residue was dissolved in 40 mL DCM and precipitated in cold diethyl ether. In a final step, the precipitate was separated by filtration, washed several times with fresh diethyl ether and dried overnight at 30 °C *in vacuo*. The resulting star block copolymer **4** was obtained as a white powder. Yield: 14 g (47 %).

^{1}H NMR (DMSO-d_6): δ 4.11 (t, 4.8 Hz; 4*), 4.02 (m; 10*), 3.98 (t, 6.6 Hz; 10), 3.51 (s; 3, 4), 3.32 (s; 2), 3.25 (s; a), 2.27 (t, 7.1 Hz; 6), 1.60–1.49 (m; 7, 9), 1.3 ppm (m; 8). The corresponding chemical structures and the proton signal assignments in the respective 1D and 2D ^{1}H NMR spectra are provided in the SI (Figure S3a and S3.1).

2.3. Synthesis of amphiphilic polymer Co-networks (5a - 5d)

5a – **5d** were synthesized by mixing DMSO stock solutions of the two star block copolymers **3** and **4** with an equimolar ratio of reactive end groups at different preparation concentrations (c_{prep} = 38, 76, 114 and 190 g L^{-1}) (see Scheme 2). The *c* values represent 0.5, 1, 1.5 and 2.5 times the overlap concentration c^* (76 g L^{-1}) assigned to sample designations **5a**, **5b**, **5c**, and **5d**, respectively. The synthesis of a representative network (**5a**) was performed as follows: 0.478 g of the DMSO solution of **3** (38 g L^{-1}) was transferred to a 2-mL glass vial (Agilent) equipped with magnetic stirrer using a 1-mL syringe. Subsequently, 0.440 g of the DMSO solution of **4** with the same concentration was added. The vial was closed and the reaction mixture was stirred at 30 °C until gelation. To keep humidity out during the reaction time, the gel was placed in a preheated desiccator with silica gel and all together in a drying oven for four days at 30 °C.

^{1}H NMR (DMSO-d_6): δ 12.40 (s; ArN*H*CO), 9.5 (br; CH_2N*H*CO), 9.19 (br; 16′), 8.42 (br; 22′), 8.15 (br; 21′), 8.00 (br; 13′), 7.82 (br; 12′), 4.32 (br; 10*′), 4.11 (s; 4*), 4.08 (br; a′), 3.97 (br; 10), 3.50 (s; 3, 4), 2.26 (br; 6), 1.54 (br; 7, 9), 1.30 ppm (br; 8). The proton signal assignments of ACN **5a** are shown in Fig. 2A.

2.4. Characterization

MALDI-TOF mass spectroscopy. Matrix-assisted laser desorption/ionization time-of-flight mass spectra (MALDI-TOF MS) of star polymers **tetra-PEG-OH**, **2**, **3** and **4** were recorded in linear positive TOF mode with a Bruker Autoflex Speed MALDI-TOF/TOF spectrometer, equipped with a Smartbeam-II Nd:YAG laser (355 nm, 1 kHz). A combination of *trans*-2-[3-(4-*tert*-butylphenyl)-2-methyl-2-propenylidene]-malononitrile (DCTB) and potassium acetate was selected as matrix and ion adductor, respectively. For a MALDI-TOF MS experiment, 8 μL of DCTB matrix solution in THF (10 g L^{-1}), 1.6 μL polymer solution in THF (2 g L^{-1}), and 0.8 μL of potassium acetate solution in ethanol (1 g L^{-1}) were mixed and dropped onto the target plate. TOF-calibration was performed using PEG reference standards between 1 and 10 kDa by PSS Polymer Standards Service GmbH, Germany.

Viscometry. A capillary viscometer of micro-Ubbelohde type I was used to determine the overlap concentrations c^* of star block copolymers **3** and **4** in DMSO at 30 °C and 45 °C. Temperature was held constant by a water bath. Stock solutions of the respective polymers were prepared and diluted to c = 15, 12, 9, 6, and 3 g L^{-1} and kept at constant temperature for 10 min prior to the measurement. The specific viscosity η_{sp} was calculated from the time *t* that a defined volume of the polymer solution needs to flow through the capillary and the corresponding time t_s for the pure solvent (1).

$$\eta_{sp} = \frac{\eta - \eta_s}{\eta_s} \approx \frac{t - t_s}{t_s} \quad (1)$$

The reduced viscosity [η_{red}] is then calculated as

$$\eta_{red} = \frac{\eta_{sp}}{c} \quad (2)$$

The intrinsic viscosity [η] is defined as [33]

$$[\eta] = \lim_{c \to 0} \frac{\eta_{sp}}{c} = \frac{1}{c^*} \quad (3)$$

and was extrapolated according to the method of Schulz–Blaschke [34].

$$\frac{\eta_{sp}}{c} = [\eta] + k_{SB}[\eta]\eta_{sp} \quad (4)$$

Volume Swelling Degree (Q_v). Q_v values of ACNs were determined in DMSO, H_2O, MTBE, $CHCl_3$, and toluene at room temperature directly after preparation (Q_{v1}) and after subsequent freeze-drying (Q_{v2}). For this purpose, all ACNs were first left to equilibrate in DMSO for two days. The ACNs were then stored in the respective solvent for another four days without prior drying. After equilibration was completed, the ACNs were weighed (Q_{v1}), freeze-dried *in vacuo*, weighed (dry weight), and placed again in the previously used fresh swelling medium for four days (Q_{v2}). The resulting gravimetrically determined equilibrium volume swelling degrees Q_v were calculated according to our previously published procedure [10,11].

High-Resolution Solution NMR spectroscopy. ^{1}H NMR spectra (500.13 MHz) were recorded on an Avance III 500 spectrometer (Bruker Biospin). DMSO-d_6 (δ(^{1}H) = 2.50 ppm) and $CDCl_3$ (δ(^{1}H) = 7.26 ppm) were

used as solvent, lock, and internal standard. Sample temperature was controlled to be constant (30 ± 0.5 °C) using a BVT-3000 instrument unless otherwise noted.

High-Resolution (HR) MAS NMR Spectroscopy. ^{1}H HR-MAS NMR spectra of **5a** – **5d** were measured in a Bruker HR MAS probe with a ZrO_2 rotor (4 mm outer diameter) and a PTFE insert (50 μL insert volume) using an Avance III 500 NMR spectrometer. For the experiments, the insert was filled with the ACNs swollen in DMSO-d_6. The spectra were recorded at 30 °C with a rotation frequency (ν_r) of 4650 Hz. The reaction efficiency p was determined from the normalized integral intensities of a signal of the reacted 2-(4-nitrophenyl)-benzoxazinone group (*H*13' of **5a** – **5d**; 8.00 ppm) and of the non-reacted 2-(4-nitrophenyl)-benzoxazinone group (*H*13 of **3**; 8.32 ppm) marked in Fig. 2, following our previously published report [10].

MQ NMR Spectroscopy. Static proton solid-state MQ-NMR experiments were used to quantify connectivity motifs and fraction of defects in a set of as-prepared ACNs (**5a** – **5d**). In cross-linked polymeric materials, a non-zero dipolar coupling between neighboring protons (the so-called residual dipolar coupling RDC) survives at long times, since network elasticity prevents an isotropic averaging of the segment orientations. The specific value of these RDCs depends on intrinsic properties such as chain length and type of repeating unit, but also on the forces from the connected chains that hold the chain in place. All studied samples were synthesized in 2-mL Agilent vials according to the synthesis protocol described above. Vials were kept immersed in a drying agent to minimize hydration effects of the DMSO-d_6 due to air humidity. All experiments were performed on a Bruker MiniSpec mq20 with a magnetic field of $B_0 = 0.47$ T (= proton Larmor frequency of 20 MHz). Temperature was regulated using a BVT-3000 unit and kept stable at $T = 25$ °C ± 1 °C. Pulse lengths were calibrated between 1.5 and 2.0 μs for 90° pulses and between 3.5 and 4.0 μs for 180° pulses. Measurements were performed using the Baum-Pines sequence [35] with incremented delays in between the pulses up to a total DQ excitation time of several hundreds of ms. The recycle delay between two subsequent scans was set to 2.0 s, which ensures a full build-up of the polymer backbone magnetization, while partially filtering-out undesired magnetization arising from non-perfectly deuterated DMSO. Due to the low number of isotropic defects (<7 % for all samples), a separation of sol content and proton-containing solvent using additional relaxation experiments (analogous to e.g. Ref. [36]) is not feasible, as the error of this procedure is on the order of the value itself. Therefore, measured defect components are always to be interpreted as a sum of sol, pending chains, and proton-containing solvent. The obtained data are analyzed using Python 3.10 and Lmfit 1.0.3 [37] with the procedures analogous to Ref. [10].

As in previous work on networks with a similar architecture [10,16,36,38], a set of three classes of connectivity motifs (SL – single link, DL – double link, HOC – higher order connectivities, see Scheme 1C) with distinct orientational degrees of freedom is assumed.[1] Each of these motifs are associated with a set of parameters (a_i, D^i_{res}, T^i_2), where a_i is its relative proton-weighted fraction, D^i_{res} is its dipolar coupling value and T^i_2, the corresponding transversal relaxation rate of the moiety. The experiment itself delivers a set of two related curves, being a relaxation-only signal (I_{ref}) and a so-called MQ build-up curve (I_{DQ}). Both curves were fitted simultaneously using the equations derived in Ref. [16] with the result of having a proton-weighted quantification of the occurrences of each moiety with a distinct mobility (a_i), as well as a rough measure of their orientational degree of freedom (D^i_{res}). Specific details on the latter are discussed in more depth in Ref. [15]. This result allows basic, but unique judgement on the structural composition and connectivity motifs of each of the gels in dependence on the synthesis parameters.

Rheology. Rheological measurements were conducted by oscillatory shear measurements on an Anton Paar modular compact rheometer of type MCR 302 (Anton Paar, Graz, Austria) equipped with a plate-plate geometry of type PP25 (diameter: 25 mm) or PP8 (diameter: 8 mm) and a solvent trap. The solvent trap was equipped with a drying agent to reduce a possible water uptake of DMSO from air. A Peltier plate was used for temperature control. ACNs were prepared in a sealed Teflon form surrounded by a drying agent according to the synthesis protocol described above at c = 38, 76, 114 and 190 g L^{-1}. The viscoelastic behavior was studied both on the fully reacted ACNs **5a** – **5d** (five days at 30 °C) and during their gelation process as a function of time in the temperature range 30–80 °C. The measurements of full-reacted ACNs were performed immediately after preparation in DMSO and then at equilibrium volume swelling degree (Q_v) in water (five days of swelling). After swelling, samples were cut to fit into the PP8. Frequency sweeps were conducted with a shear amplitude of $\gamma = 0.5$ % and in the range of ω = 1–100 rad s^{-1}.

3. Results and discussion

In this study, amphiphilic star block copolymers were prepared which already contain both components (PCL, PEG) in one star, see Scheme 3B. This complements our previous work on A_4B_4-type ACNs, where hydrophobic PCL and hydrophilic PEG tetra-arm star polymers served as building blocks [10,15,17], see Scheme 3A. The current synthesis strategy allows to encode the amphiphilic character in the precursor polymers. This guarantees the miscibility of the components on the length scale of individual stars, while the physics of block copolymers can be utilized to structure the material on demand prior to gelation.

In the following, we first explain the synthesis strategy and structural analysis of 2-(4-nitrophenyl)-benzoxazinone- and amino-terminated tetra-PEG-*b*-PCL star block copolymers, **3** and **4**, respectively. This also includes the determination of the overlap concentration c^* of **3** and **4**, and the understanding between the polymer blocks (PEG, PCL) in the synthesis solvent DMSO (interaction parameters). The results are summarized in Tables 1 and 2. Then, the formation of ACNs by heterocomplementary reaction of **3** and **4** and analysis of the co-networks **5** by HR MAS (high-resolution magic-angle-spinning) and MQ (multiple quantum) NMR spectroscopy in DMSO as well as swelling experiments in different solvents are described. Finally, both the solvent-dependent viscoelastic behavior of ACNs and their temperature- and concentration-dependent gelation process determined by rheological studies are discussed. The results are summarized in Tables 3 and 4.

3.1. Synthesis and structural analysis of tetra-PEG-b-PCL star block copolymers 3 and 4

The synthesis steps of star block copolymer **3** and **4** shown in Scheme 1A were monitored by NMR spectroscopy and MALDI-TOF MS. Initially, hydroxy-terminated star block copolymer **2** with a theoretical number average molar mass of 10.4 kg mol^{-1} was prepared by ROP of 46 equivalents of ε-caprolactone (ε-CL) according to the "core-first" approach with one equivalent of **tetra-PEG-OH** (related to the hydroxy group) as the initiating core. With this synthesis strategy, monodisperse tetra-PEG$_{116}$-*b*-PCL$_{44}$ star block copolymer **2** with the targeted number of ε-CL repeating units per arm (n = 11, see Table 1) was achieved as determined by ^{1}H NMR end group analysis (see SI Figure S1). SI Figure S2b depicts the ^{1}H NMR spectrum of star polymer **2**. Absence of the hydroxy signal *H*5 at 4.52 ppm indicates a quantitative esterification

[1] A special aspect of our network architecture is the suppression of pending loops and all other cyclic structures that are made of an odd number of network strands [13,14]. This leads to a clearer separation of the RDC of double links from the remaining signal of the elastic part of the network, see e.g. the green data set in Fig. 3 of Ref. [51]. After elimination of the RDC of all odd i_{min} in this Figure, the difference between the RDC at $i_{min} = 2$ (the double links) and the remaining $i_{min} \geq 4$ becomes more than a factor of two and thus, these signals can be discerned. For more conceptual insights, the reader is referred to Ref. [58].

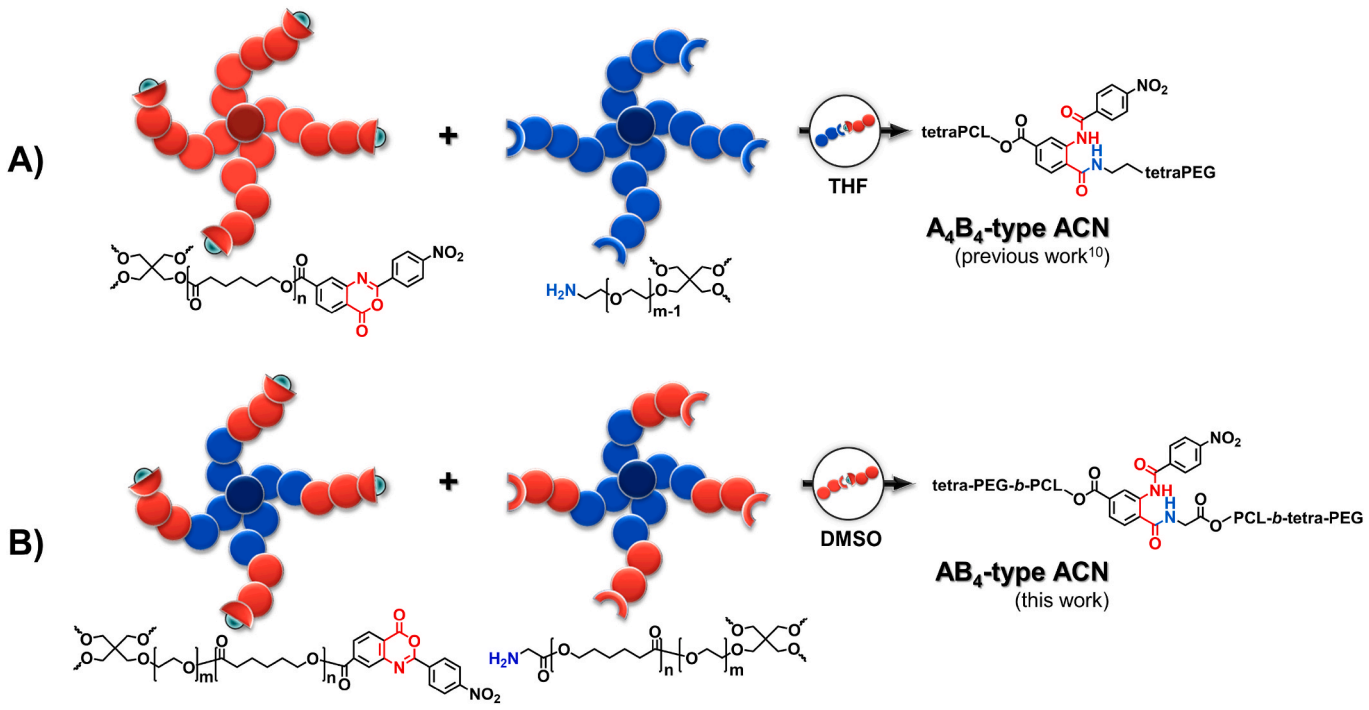

Scheme 3. Comparison of two synthesis strategies for the formation of ACNs with model structure from A) homo-PEG and -PCL star polymers as described in our previous work [10] and B) PEG-*b*-PCL star polymers of the present work.

Table 1
Molecular characteristics of star polymers **1**, **2**, **3**, and **4**.

Star polymer	m_{PEG}[a]	n_{PCL}[a]	w_{PEG}[b] (%)	w_{PCL}[b] (%)	M_n[c] kg mol^{-1}	M_n[d] kg mol^{-1}	$Đ$[d]	$c^*_{30°C}$[e] (g L^{-1})	$c^*_{45°C}$[e] (g L^{-1})
PEG	29	–	97.4	–	5.2 ± 0.1	5.3 ± 0.1	1.02	–	–
2	29	11	49.8	48.9	10.3 ± 0.2	10.1 ± 0.6	1.04	–	–
3	29	11	44.6	43.9	11.4 ± 0.2	10.5 ± 0.7	1.04	74.2 ± 0.4	76.2 ± 0.9
4	29	11	48.7	47.9	10.5 ± 0.2	11.4 ± 0.7	1.03	77.2 ± 0.3	77.9 ± 0.4

[a] Number of monomer units of the PEG block and the PCL block per arm, respectively, based on ^{1}H NMR spectroscopic analysis (see SI Fig. S1 and comments).
[b] Proportions of the core and the end groups were also taken into account in the calculation.
[c] Determined by ^{1}H NMR spectroscopy.
[d] Determined by MALDI-TOF MS, $Đ$ = Dispersity (M_w/M_n).
[e] Overlap concentration determined by viscometry with Schulz-Blaschke regression model in DMSO (see Fig. 1).

Table 2
Hansen estimates of the interaction parameter χ based upon different data [40, 41]for the solubility parameters. The calculation and all parameters are described in Section 7 of the SI.

X estimates of DMSO for	25 °C	80 °C	Ref.
PEG	0.11	0.09	[40]
PEG	0.33	0.28	[41]
PCL	0.43	0.42	[40]
PCL	0.60	0.58	[41]

Table 3
Characteristic structural parameters of the synthesized ACNs **5a – 5d** based on the cross-linking of star block copolymers **3** and **4** in DMSO at 30 °C.

ACN	c_{prep} (g·L^{-1})	c_{prep}/c^*	φ_0	p[a]	f_{def}[b]
5a	38	0.5	0.034	≥0.90	0.07
5b	76	1	0.068	≥0.95	0.03
5c	114	1.5	0.102	≥0.95	0.03
5d	190	2.5	0.170	≥0.95	0.01

[a] Degree of conversion p determined by ^{1}H HR MAS NMR spectroscopy after removal of the sol fraction and swollen in DMSO-d_6.
[b] Isotropic defect fraction determined by ^{1}H MQ NMR spectroscopy.

of the PEG hydroxy groups. To introduce the above-mentioned terminal groups, the hydroxy groups of **2** were then modified with **Fmoc-Gly-OH** and 2-(4-nitrophenyl)-benzoxazinone-based compound **1**, respectively. By comparing the stacked ^{1}H NMR spectra of **2** and **3** in ESI Figure S2 and of **2** and **4** in ESI Figure S3, the complete disappearance of the proton signal *H*11 at 4.30 ppm of **2** demonstrated a quantitative conversion of the hydroxy groups to the respective end groups. Furthermore, the Fmoc group was successfully cleaved, as indicated by the absence of proton signals in the aromatic region of **4** at 7.32–7.89 ppm (see ESI Figure S3a).

MALDI-TOF mass spectra of **tetra-PEG-OH, 2**, **3** and **4** were measured to determine the molar masses of the stars (by the mass to charge ratio) and their relative differences (see ESI Figure S4). Between the mass peak apexes of **1** and **2**, a relative difference of $m/z \approx 4700$ was observed, corresponding to a relative difference in number average molar mass of 4.9 ± 0.2 kDa which agrees to the total number of PCL repeating units per tetra-PEG-core found by solution NMR spectroscopy. Star block copolymer **3** showed a relative difference between the peak apexes of $m/z \approx 1100$ to its predecessor **2**, which corresponds to the molar mass of the four oxazinone terminal groups. The relative increase

Table 4
Storage moduli and equilibrium swelling degrees in DMSO and H_2O of ACNs **5a** – **5d** synthesized in DMSO at 30 °C.

ACN	φ_0	$G'^{a)}$ (kPa) DMSO	H_2O	Q_{v1} DMSO	H_2O
5a	0.034	0.69 ± 0.02	29.00 ± 1.07	33.6	10.2
5b	0.068	5.18 ± 0.24	72.65 ± 0.93	18.2	6.2
5c	0.102	9.74 ± 0.41	105.3 ± 4.35	13.0	4.9
5d	0.170	29.87 ± 1.39	152.3 ± 1.67	9.2	3.8

[a] Storage moduli in DMSO (as-prepared state) and in H_2O at equilibrium swelling at $T = 25$ °C.

in m/z of star block copolymer **4** to its precursor **2** (between peak apexes) of about m/z 1050 is significantly higher than expected. For the conversion of hydroxy groups to amino groups (see Scheme 1), an increase in molar mass of 228 g mol^{-1} is expected. The distinctly higher increase in molar mass can be explained by chemical adduction of molecules of the MALDI-matrix DCTB to free terminal amino groups, as reported earlier [39]. This effect indicates indirectly the existence of free terminal amino groups, but it was not further investigated since it is beyond the scope of this work.

For understanding the behavior of the star block-copolymers in solution, the interaction between the polymer blocks and DMSO needs to be understood. Table 2 contains an estimate for the interaction parameters of PEG and PCL with DMSO based upon literature data on the solubility parameters [40,41] and the Hansen approach [41].

The computations and the key parameters used are summarized in Section 7 of the supporting information. Table 2 indicates a significant dependence of χ on the available data for the solubility parameters. Therefore, we compare with other literature data for testing the quality of the interaction parameter estimates. According to Qin and Wu [42], 80 kDa PCL does not dissolve in DMSO at room temperature, but it dissolves at 80 °C. Since the molar mass of the PCL is rather large and the temperature dependence of the interactions between DMSO is expected to be weak, see Table 2, this indicates that the parameters of Ref [41]. for PCL agree better with the experiment. Thus, DMSO is presumably a weakly poor solvent for PCL. DMSO is a strongly hygroscopic solvent and it absorbs significant amounts of water from air during typical times where experiments are conducted [43]. Since water is a non-solvent for PCL, this effect develops a significant impact on the solubility of the PCL over time. This point is even utilized for the spinning process of PCL fibers from a solvent mixture containing DMSO: humidity of the surrounding air is the control parameter for the microstructure and the porosity of the resulting PCL fibers [44,45]. We were not aware of this complication when designing our experiments. Instead, we expected from Ref [[46]]. that our star block-copolymers should simply be soluble in DMSO, which is apparently not the general case, in particular, when a contact between solvent and air cannot be avoided entirely and when long measurement times are involved (e.g. rheology during cross-linking, frequency sweeps for rheology, etc…) . The corresponding data are discussed in the following sections with particular care. The experiments in the preceding sections, on the other hand, were conducted under conditions where an impact of humidity can be safely ignored.

The investigations with NMR spectroscopy and MALDI-TOF MS show that star block copolymers **3** and **4** are characterized by a high molecular uniformity and functionality, which is a prerequisite for the synthesis of model networks. Another important aspect is the knowledge of the overlap concentrations c^* of the stars, since only above this concentration, homogeneous space-filling networks can be expected. The overlap concentration can be estimated from the intrinsic viscosity $[\eta]$ [2,17], see equation (3). The intrinsic viscosity and the overlap concentration of a polymer depend on temperature and the solvent quality [47]. For tetra-PEG- and tetra-PCL-stars, overlap concentrations c^* in different solvents were analyzed in our previous publication [10]. In the present study, dilution series of the star block copolymers **3** and **4** in DMSO were used to determine $[\eta]$ at 30 and 45 °C following the protocol of preceding work [10]. According to the Schulz-Blaschke equation (4), $[\eta]$ values for **3** and **4** were obtained by linear extrapolation of the reduced viscosities η_{red} to the zero specific viscosity η_{sp} (see Fig. 1). The resulting estimates for the overlap concentration c^* are shown in Table 1. These results indicate that the quality of DMSO for star polymers **3** and **4** decreases with increasing temperature in contrast to the expectation, see Table 2. Apparently, the higher humidity provided by the water bath at 45 °C causes already a somewhat lower solubility of the star blocks in DMSO inside the viscosimeter. Thus, the data at 30 °C provide effectively an upper bound for the overlap concentration at zero humidity. This point is also evident from the Schulz-Blaschke constants as determined from the slope of the data. These refer to a solvent quality in the range of theta to slightly poor solvent conditions [48], while a net solvent quality between good and theta can be expected from Table 2. Since polymers **3** and **4** differ only in their end-groups, the higher slope of the data for **3** indicates a comparatively lower solubility of the oxazinone end-groups in DMSO. But as the intrinsic viscosity is not largely modified, the solubility appears to be still good enough to prevent an aggregation of **3**.

3.2. Synthesis and structural analysis of ACNs 5a – 5d

The syntheses were carried out in solution (gels) by heterocomplementary coupling of star block copolymers **3** and **4** at equimolar ratio of the terminal groups and varying preparation concentration c_{prep} (see Table 3) within four days at 30 °C. DMSO was chosen as a solvent because both star block copolymers are soluble in it [46]. In addition, DMSO has a high boiling point of 189 °C, which prevents evaporation of the solvent during rheological measurement. Toluene as a potential solvent also meets the above conditions, but surprisingly, no

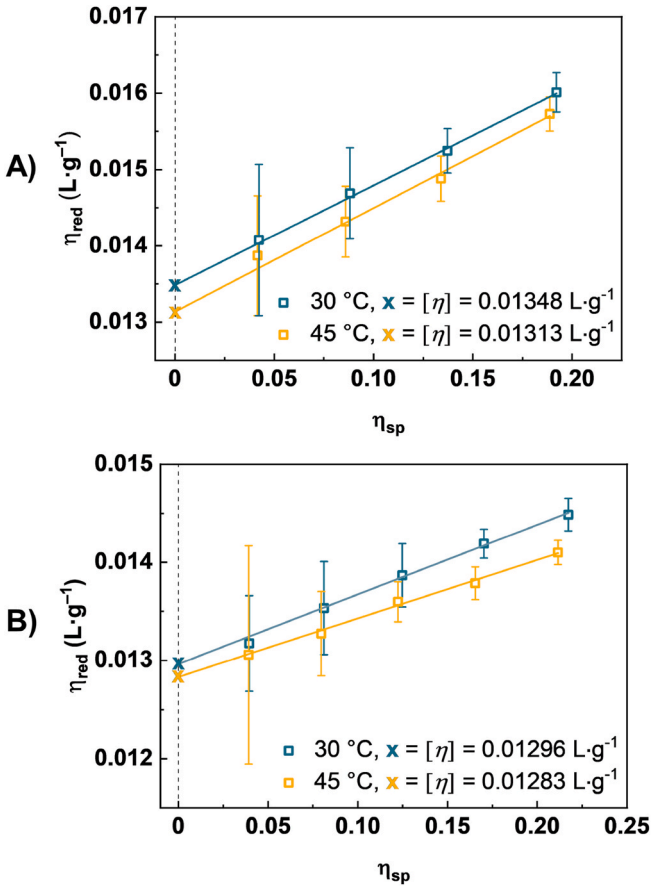

Fig. 1. Schulz-Blaschke plots of star polymer **3** (A) and **4** (B) in DMSO measured at $T = 30$ and 45 °C [34].

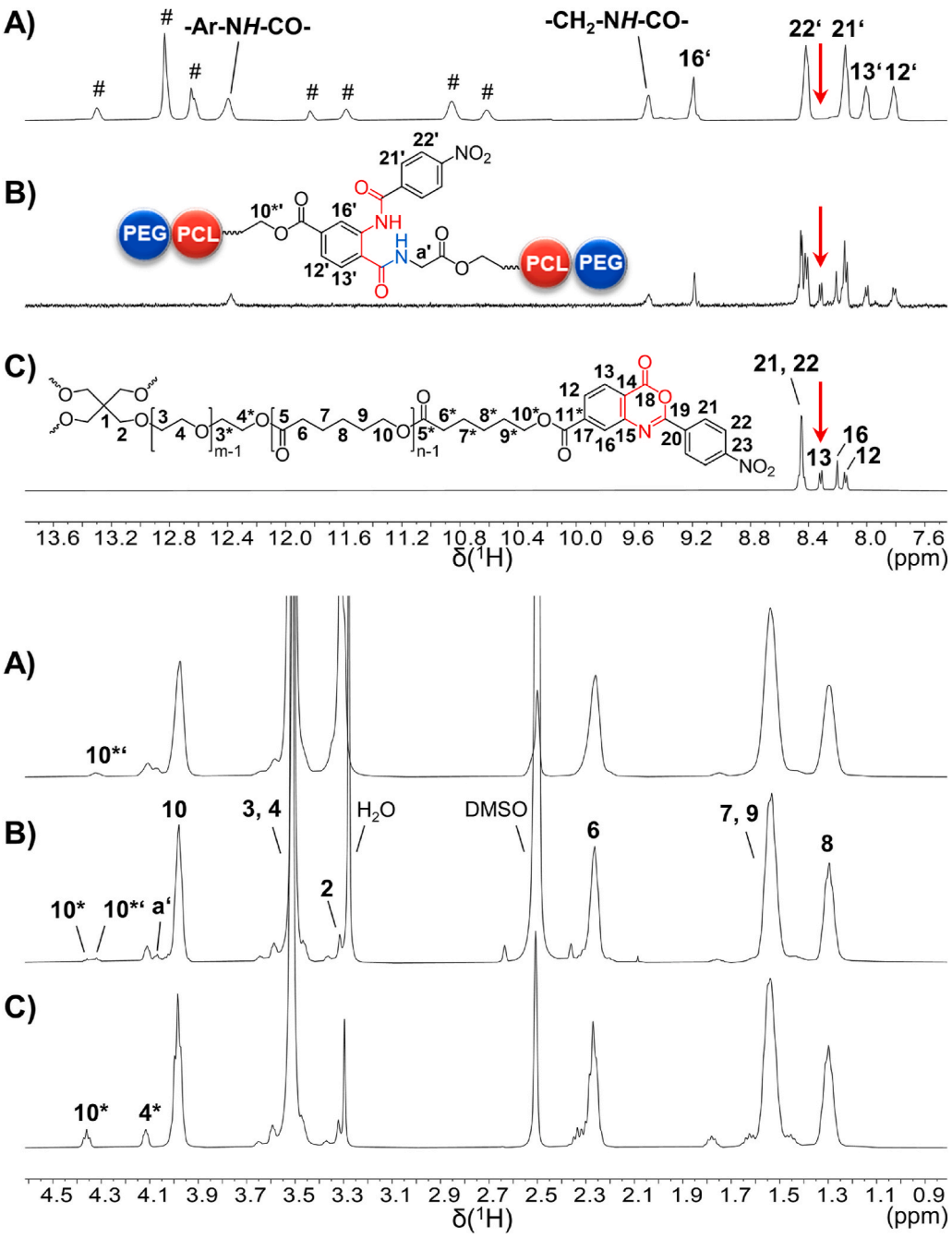

Fig. 2. ^{1}H NMR spectra (regions) in DMSO-d_6 at 30 °C of A) **5a** measured with a HR MAS NMR probe at equilibrium swelling, B) during reaction after 45 min at a 2-(4-nitrophenyl)-benzoxazinone conversion of ~50 % and C) of star block copolymer **3**. The red arrow indicates unreacted 2-(4-nitrophenyl)-benzoxazinone groups (*H*13), which have almost completely disappeared in A). Symbol # denotes spinning side bands of the intense aliphatic signals. (For interpretation of the references to color in this figure legend, the reader is referred to the Web version of this article.)

gelation was observed in this solvent within 24 h. In DMSO, gelation was observed within 1 h after mixing the stoichiometric stock solutions and continued for a total of 4 days to generate the highest possible conversion. The characteristic parameters of the networks synthesized at different c_{prep} are summarized in Table 3. The sample designations **5a** – **5d** reflect the different preparation conditions of the ACNs. For different analytical methods, several samples with the same designation were prepared, for instance, when observing gelation in situ in the rheometer. Since the applied network synthesis was shown to be highly reproducible [10], we expect comparable results for samples with the same preparation conditions.

First, the degree of conversion *p* was determined by ^{1}H HR MAS NMR spectroscopy of the sol-extracted ACNs **5a** – **5d** swollen in DMSO-d_6 as described previously [10,12]. It is noteworthy that the synthesis was performed in DMSO-d_6 and that the samples were not dried before measurements to avoid possible post reactions. Fig. 2 shows the ^{1}H NMR spectra of **3** (A), a mixture of **3** and **4** after 45 min of cross-linking (B), and ACN **5a** after 4 days of cross-linking (C) at 30 °C DMSO-d_6. Decisive for the determination of the degree of conversion are the terminal group signals, the intensity of which disappear during the reaction. Accordingly, the proton signals *H*13 of star polymer **3** and *H*13′ of the resulting ACN **5a** were used to calculate *p* of **5a** – **5d**. It is clearly visible that the *H*13 signal of the 2-(4-nitrophenyl)-benzoxazinone terminal groups in Fig. 2c disappeared almost completely in Fig. 2a (red arrow). Instead,

new signals appear that can be assigned to the newly formed benzamide linkage between the PCL blocks in the network (e.g. *H*13'). The resulting values of *p* in Table 3 are distinctly higher than in classical tetra-PEG gels [49] and comparable to our preceding work [10]. Due to the broadened shape of signal *H*13 caused by an extreme shortening of T_2 at the sol-gel transition [10], the *p* values even tended to be underestimated.

Another major concern was to investigate the topological microstructure of the ACNs. In our previous publication [10], the static low-field ^{1}H MQ NMR spectroscopy has proved to be a powerful tool to quantify structural heterogeneities (e. g. sol fraction) as well as the chain connectivities of ACNs based on tetra-PEG and tetra-PCL synthesized in a similar manner as described here. Comparable studies were performed on ACNs **5a** - **5d** swollen in DMSO-d_6. The results are summarized in Table 3 (defect fractions f_{def}), Fig. 3 (connectivity fractions), see also SI Section 5 Table S5.

The defect fraction includes unbound chains and dangling chain ends in the network. The results are in accord with the data on conversion and show a concentration dependence that results from the smaller number of suitable reaction partners for the hetero-complementary coupling with decreasing concentration. The connectivity fraction indicates how many arms of a star are connected to a neighboring star, illustrated in Scheme 1C. One distinguishes between single links (SL), double links (DL) and higher order connectivities (HOC). In a perfect network, only single links would occur. However, due to the statistical course of the cross-linking reaction, the formation of DL and HOC cannot be prevented. Examples for the connectivity distribution of single and double links in homopolymer model networks made of star polymers are given in the literature [13,16].

For ACNs **5a – 5d**, we find the expected trend of a decreasing isotropic defect fraction (from 7 % at $c_{prep} = 0.5\ c^*$ to 1 % at $c_{prep} = 2.5\ c^*$) that is accompanied by a consistently increasing fraction of single links (SL) (4 % at $c_{prep} = 0.5\ c^*$ to 40 % at $c_{prep} = 2.5\ c^*$), as well as a strongly-increasing average residual dipolar coupling (RDC) (9 Hz at $c_{prep} = 0.5\ c^*$ to 109 Hz at $c_{prep} = 2.5\ c^*$) see Table S5 in the SI. The decrease in isotropic defect fraction with increasing c_{prep} is roughly in agreement with the data on conversion (see Table 3). While the general behavior aligns well with our previous work, we find the specific values at $c_{prep} = 0.5\ c^*$ rather unexpected, as these suggest that this sample contains nearly no single links and only a rather small number of double links. We note, that at $c_{prep} = 0.5\ c^*$ the distinction between components of unique RDCs is barely possible due to a high fraction of low orientations that are typically assigned to more complex structures, defects, or double links.

There are two possibilities how an enhanced portion of low orientation can arise inside our networks. First, the viscosity measurements showed a significantly larger Schulz-Blaschke constant for compound **3** as compared to **4** indicating a poor solubility of the 2-(4nitrophenyl)-benzoxazinone terminal group in DMSO. Possible associations of terminal groups attached to the same star lead to an apparent double link between star center and the location of the association. In effect, the analysis of the NMR data will overestimate the amount of double links and more complex associations mostly at the expense of single links. Second, a clear distinction between single and double links requires that the networks are far from the gelation threshold. Otherwise, there will be a significant portion of star polymers that connect in effect only two other stars introducing longer strands with correspondingly lower orientation. Such structures will be misinterpreted then as double links, more complex structures or even defects.

In order to understand, which of these processes is more relevant for interpreting the experimental data, we compare with the simulation data of Ref. [15] providing estimates for the amount of double links in comparable systems without associations. For comparison, data were chosen near 0.5*c** at a slightly higher conversion of $p = 0.95$ as compared to the experiment. The reason for this choice is that samples at low concentrations are closer to the critical concentration for gelation where the length of virtual chains modeling the elasticity of the surrounding network diverges, and consequently, different motifs become indistinguishable. For more certainty, we analyzed the network structure to determine single links (SL), double links (DL), higher order connectivities (HOC), and elastically inactive defects. For these different kinds of connections, the distributions of the vector order parameters are shown in Fig. 4.

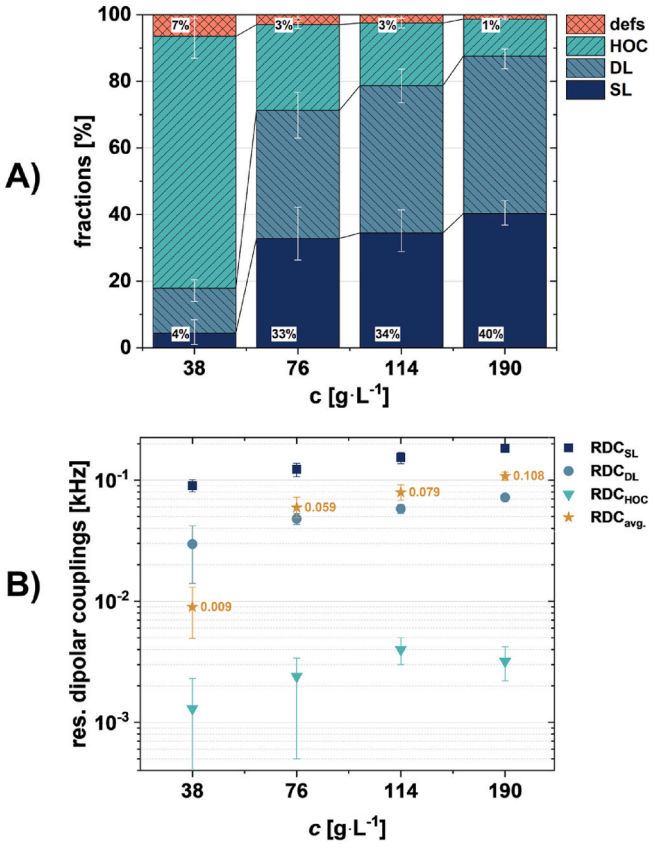

Fig. 3. Connectivity fractions (A) and RDC value (B) of ACN **5a – 5d** synthesized at different concentrations (76 g L^{-1} ~ *c**) in DMSO-d_6. (SL – single link, DL – double link, HOC – higher order connectivities, defs – isotropic defects).

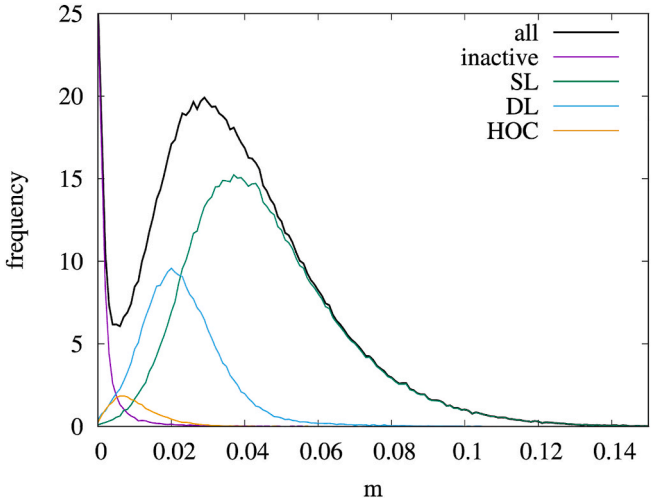

Fig. 4. Distribution of the vector order parameters of different connectivity types at 0.5*c** as determined from computer simulations. The weight fractions of single links (SL), double links (DL), higher order connectivities (HOC), and elastically inactive defects are 68.2 %, 23.2 %, 2.4 %, and 6.2 %, respectively. Data were computed from the network with N = 43 described in preceding work [15].

The simulation data in Fig. 4 show that higher order connectivities play no role at 0.5c^* and thus, for all samples of our study. This leaves only possible associations on the time scale of the NMR experiments as explanation for the experimental data. The vector order parameter is proportional to the RDC that is measured in the experiments, see Ref [[50]]. for more details. At the lowest concentration, the simulation data show that the peak positions of the different contributions differ by a factor of two in the RDCs, which is on the edge of being separable in the experiment, see Ref. [16]. The RDC is proportional to the elastic contribution per strand in the entanglement free limit. For a double link inside an otherwise perfect network, a ratio of 8:3 between SL and DL is, expected theoretically, which is found in good approximation in the experiment and in simulations at higher concentrations [16,51]. At $c_{prep} > 0.5c^*$, the SL fractions are consistently below the data of the simulation (>60 % SL fraction), while being on-par with the values for the amphiphilic copolymer networks characterized in our previous work. In combination with the large Schulz-Blaschke constant of compound 3 (which differs from compound 4 only in the terminal group), we have now high confidence that a possible association of the 2-(4-nitrophenyl)-benzoxazinone terminal group in 3 is perturbing the assignment of single and double links.

3.3. Swelling properties of ACNs 5a - 5d

Equilibrium volume swelling degrees Q_v of ACNs **5a** – **5d** were investigated in solvents of different quality with respect to PEG and PCL (see Fig. 5). In Fig. 5A, Q_v was determined both directly after synthesis without drying the samples (Q_{v1}) and after freeze-drying with subsequent swelling (Q_{v2}). In the first case, the data at and above the overlap threshold are described by a power-law $Q \sim \varphi_0^{\gamma}$ with an exponent $\gamma = -0.76 \pm 0.05$ which disagrees with our previous work [15] and the predictions by Flory-style mean-field scaling models [52,53] for swelling in a good-solvent. In particular, for the samples synthesized near c^* ($\varphi_0 = 0.068$) and especially below c^*, an increase of the equilibrium swelling degree is observed as compared to our preceding work [10], which indicates a somewhat lower extent of reactions or an additional enhancement of double links that contribute less to the shear modulus [51]. The higher concentration of not yet reacted end groups upon drying enhances the formation of additional bonds in a different state of strain [10,14]. In consequence, a fair drop in the equilibrium degree of swelling is observed after the first drying step. This has already been observed in our previous studies on ACNs based on tetra-PEG and tetra-PCL [10].

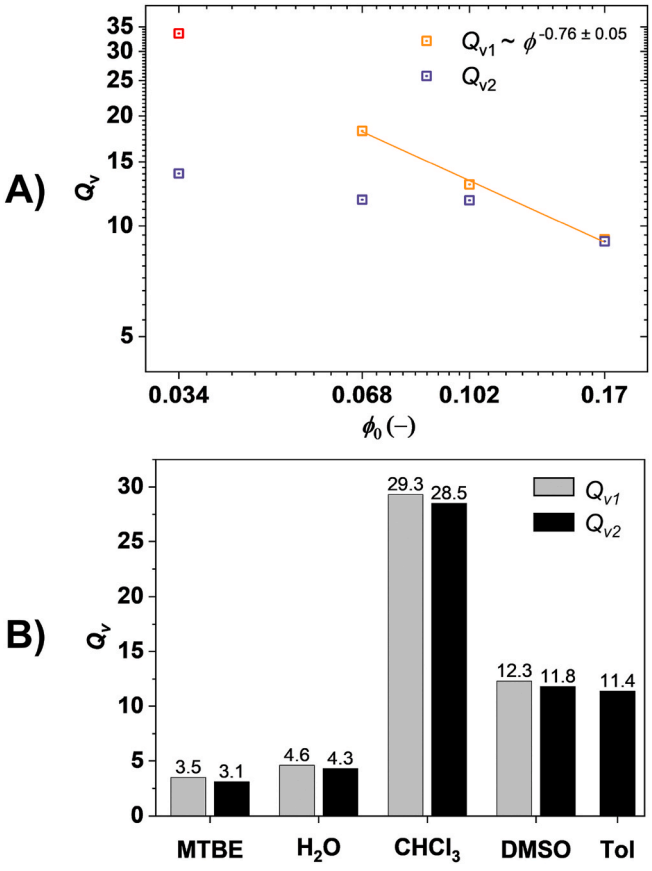

Fig. 5. Equilibrium volume degree of swelling Q_v (Q_{v1} directly measured after preparation and Q_{v2} measured after freeze-drying and re-swelling) A) as a function of polymer volume fractions at preparation state φ_0 in DMSO with a power-law fit $Q \sim \varphi_0^{\gamma}$ at $\varphi_0 \geq 0.068$ and B) of 5c in dimethyl sulfoxide (DMSO), toluene (Tol), methyl-*tert*-butyl ether (MTBE), chloroform ($CHCl_3$), and H_2O.

To demonstrate the amphiphilic nature of the networks, swelling tests in solvents of different polarity were performed on five batches of ACN **5c** synthesized at 1.5c^*. The results are shown in Fig. 5B. Here, the measurements refer to an analysis both directly after synthesis in DMSO with swelling in the respective solvent (Q_{v1}) and after freeze-drying with subsequent swelling (Q_{v2}) as described in the **Experimental Section**. The largest Q_v was observed in $CHCl_3$, which can be attributed to good solvent quality for both PEG and PCL. The equilibrium degree of the first swelling in chloroform is comparable with our expectations based upon Ref. [10] indicating a similar reaction efficiency in DMSO as in chloroform. The lowest Q_v was observed in H_2O (close to a theta solvent for most concentrations of PEG and a non-solvent for PCL [54]) and MTBE (poor solvent for both). From the bar chart in Fig. 5B, it can also be seen that **5c** shows similar swelling degrees in DMSO and toluene. In this case, toluene is the better solvent for PCL [10], while these roles are reversed for DMSO. In addition, due to the structural similarity, toluene is suspected to contribute to the solvation of the benzamide groups by π-π interactions, which is similar to our discussion of linker associations in DMSO. Thus, the agreement in the average degree of swelling in DMSO and toluene is not in conflict with our RDC data.

3.4. Viscoelastic behavior of ACNs 5a – 5d

In the following, the results of oscillatory shear rheological measurements of **5a** – **5d** in the as-prepared state in DMSO, at swelling equilibrium in H_2O, and during the gelation process of star polymer **3** and **4** at different gel preparation conditions are discussed. The measurements on as-prepared samples were performed after a reaction time of five days in DMSO. Details about the sample preparation are described in the Experimental Section. Additionally, measurements were made on samples swollen in water. The elastic contributions of the storage moduli G' and their corresponding swelling degrees in equilibrium Q_{v1} in both solvents are listed in Table 4.

An example of an as-prepared gel sample as well as the rheological frequency sweeps of **5a** – **5d** in DMSO are shown in Fig. 6. In all cases, a dominance of the elastic behavior ($G' > G''$) is observed, which is typical for the plateau regime of a polymer network that is stable on the time scale of the experiment. When repeating the frequency sweeps, sometimes, a small drift of the data was observed as a function of time (not shown). Moreover, a sample left overnight in the rheometer turned opaque indicating a slow water uptake from air during the measurements despite of using a solvent trap equipped with a drying agent. A reduced solvent quality for PCL due to the presence of water induces smaller equilibrium strand sizes and ultimately a micro-phase separation, both enhancing the modulus of the samples. Therefore, our modulus data provide only an upper bound for the data in a water free sample. As compared to our preceding paper [10], the modulus at c^* is about twice as large while this difference grows to a factor of about 3 at 3c^*. The remarkable point is that the equilibrium degree of swelling does not follow this trend see Fig. 5B of the present work (toluene and DMSO

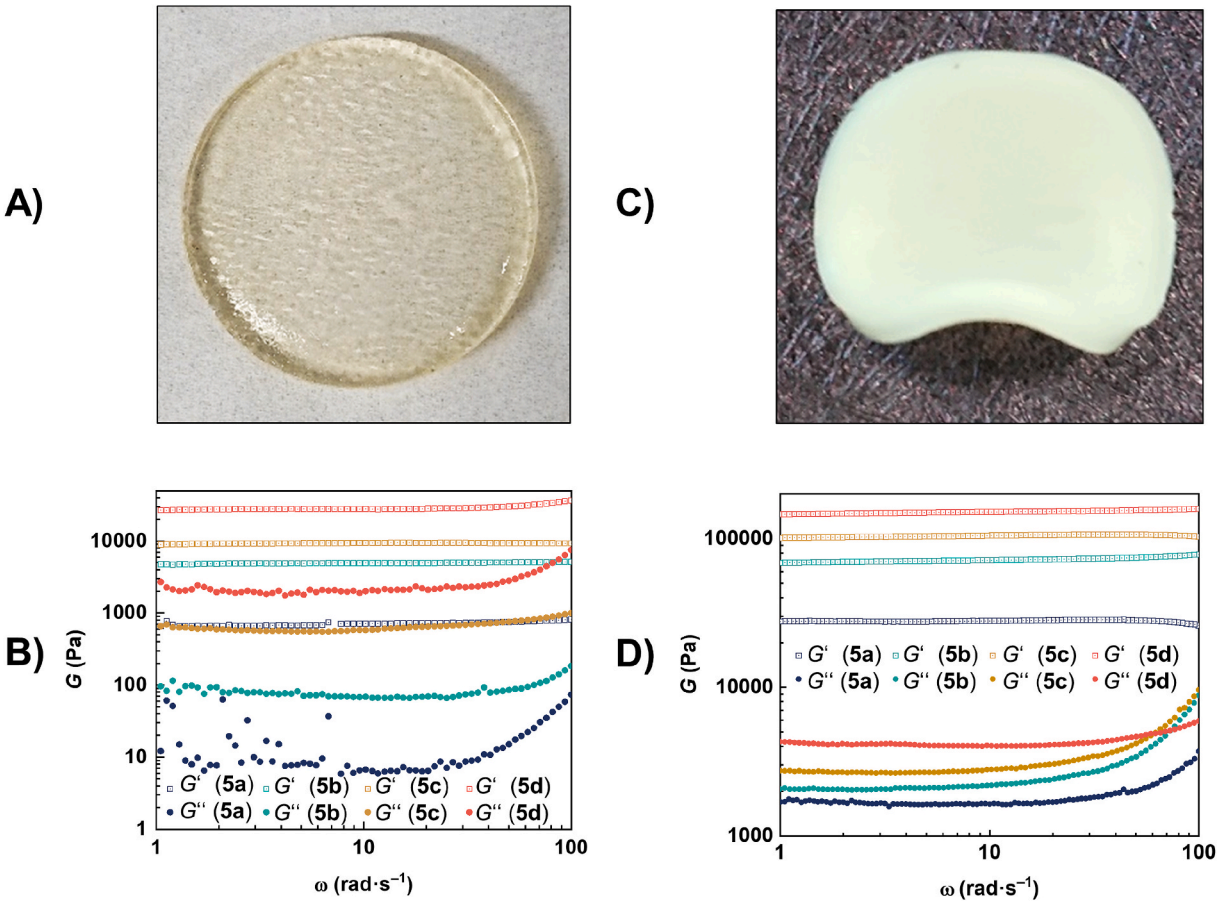

Fig. 6. A) Appearance of an as-prepared gel sample, B) rheological frequency sweeps of **5a** – **5d** in DMSO at preparation conditions, C) Appearance of a gel sample after exchange of DMSO with water, D) rheological frequency sweeps of **5a – 5d** in H_2O at swelling equilibrium.

produce equivalent results, i.e. equivalent net interaction parameters) and Fig. 5 of Ref. [10] (the interpolated (to 1.5c^*) equilibrium degree of the second swelling in toluene is around 11 and equivalent to the data in Fig. 5B).

A better insight into this puzzling situation is obtained when analyzing the time-dependent rheological measurements performed during cross-linking under the same reaction conditions as described in Table 3. The respective time evolution curves of G' are shown in Fig. 7, see also SI Section 6 Table S6. We observe a two-step increase of the storage modulus at low temperatures, while at higher temperatures, there is only a one step increase. In the latter case, the single process must describe the gelation of the samples. According to the temperature dependence of the processes, the second process at lower temperatures in Fig. 7B refers to cross-linking, while an explanation of the nature of the additional first process requires further tests. First, rheological measurements of pure solutions of **3** and **4** do not reproduce the effect. Thus, the effect arises only as the consequence of the cross-linking reactions. Cross-linking glues two PCL sections together. We argue that the longer PCL sections after cross-linking associate in the DMSO solution. This association is probably enhanced by the coupling terminal 2-(4-nitrophenyl)-benzoxazinone group itself that lowers the solubility of the star polymers, see section viscosity measurements. This hypothesis is the same as used to explain the MQ-NMR data and it allows to remove all other conflicting observations:

First, it is well established [55,56] that the concentration of the associated groups grows with concentration. Thus, we can expect an enhancement of modulus at preparation conditions that grows with concentration through additional contributions from sticky chain sections. Second, reversible networks do not resist swelling in the limit of very long times. Thus, we expect no impact on the equilibrium degree of swelling beyond a concentration dependent renormalization of the net interactions between the polymers and the solvent. The renormalized interactions lead to a stronger concentration dependence of the equilibrium degree of swelling as observed in Fig. 5a. Taking both points together, permanent networks with sticky chain sections can develop a higher modulus at preparation conditions even though the equilibrium degree of swelling is nearly identical to a permanent network without such sticky chain sections.

The time dependent rheology data on G’ provides additional interesting insights. The disappearance of the first gelation process does not indicate a complete disappearance of all the associations. It only shows that there are too little associations to drive the system through gelation prior to the gelation of the permanent network structure itself. Moreover, the stability of the associations must exceed 1 s at the measurement temperature, if the second process is visible. The frequency sweeps show that the associations are stable over 1 s at 30 °C while NMR indicates stable associations up to 1 ms at 80 °C. Both are not in conflict with each other and allow for a rearrangement of the associations on the time scale of the swelling experiments (days).

After preparation, gels **5a - 5d** were swollen to equilibrium in excess H_2O without an intermediate drying step. The gels appear white (see Fig. 6C). Since preliminary SAXS and SANS measurements on the previous series (unpublished) indicate that crystallization of the PCL phase is strongly suppressed in such networks, light scattering on PCL crystals can be ruled out as the cause of the white color. This assumption is supported by studies on PEG-PCL block copolymers in water, which indicate a suppressed crystallization of PCL by increasing curvature of the surface between PEG and PCL [57]. Therefore, we attribute the

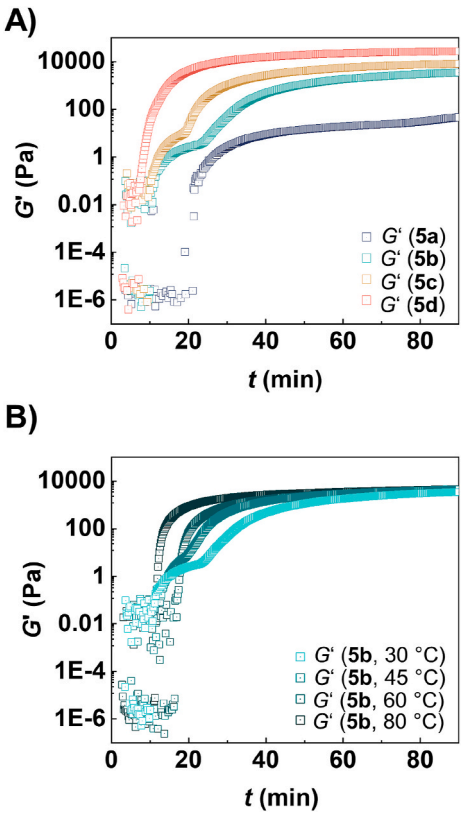

Fig. 7. In situ measurements of the storage modulus as a function of time during gelation for A) samples **5a** to **5d** at different polymer volume fractions, see Table 3, and B) sample **5b** at different temperatures from 30 to 80 °C.

white color to heterogeneous aggregates of the PCL domains.

The equilibrium degree of swelling of these samples was determined gravimetrically and is summarized in Table 4. The equilibrium degree of swelling of samples **5b - 5d** prepared at and above the overlap threshold scales as $Q \sim \varphi_0^{\gamma}$ with $\gamma = -0.53 \pm 0.03$. The elastic modulus of these samples is several times higher in comparison to the modulus in DMSO. For a first glimpse on the physics of this process, let us consider the ratio of the modulus of a homogeneous network before and after a change in sample volume. For this modulus ratio, the following dependence on the polymer volume fraction is expected [48] in good ($\nu = 0.588$) and theta ($\nu = 1/2$) solvent $G(\varphi)/G(\varphi_0) \approx (\varphi/\varphi_0)^{1/3+(2\nu-1)/(3\nu-1)}$, when swelling from a preparation state to a swelling equilibrium with $\varphi < \varphi_0$. For our samples, however, a change in interactions and chain conformations drives the system to a swelling equilibrium characterized by $\varphi > \varphi_0$. Our rheology–data for samples **5b - 5d** prepared at and above c^* are in accord with an exponent of 2.2 ± 0.5 for the modulus ratio. Here, the network elasticity has to work against the osmotic pressure of the sample and additional constraints arising from the interphase between swollen and phase separated polymers. The new equilibrium degree of swelling reflects the sum of all these constraints on the free energy. The osmotic pressure in homogeneous samples in good and theta solvents scales [48] as $\Pi \approx \varphi^{3\nu/(3\nu-1)}$, which is not largely different from the observed increase in modulus. This observation could be useful for developing a model for the elasticity of amphiphilic gels in a selective solvent.

4. Conclusion

Following our earlier work on the synthesis of ACNs based on tetra-PEG and tetra-PCL stars [10], we synthesized networks in which the hydrophobic and hydrophilic components were already contained in all individual stars. The latter is the major difference to the preceding work allowing for a possible structuring of the networks in a block copolymer morphology prior to the synthesis. As in the preceding paper, the hetero-complementary 2-(4-nitrophenyl)-benzoxazinone/amine reaction has proved to be very effective to link the star polymers. Apart from the resulting differences in the arrangement of the polymer blocks, the new ACNs do not differ from the ACNs in Ref. [10] in terms of linking group, degree of polymerization of the network strands, and the volume fraction of the amphiphilic and hydrophilic components. Since the two block stars 4 and 5 are structurally identical except for their end groups, the small difference in their solubility can be attributed to the end groups. A synthesis in toluene did not produce networks within 24 h, therefore, DMSO was used as a solvent. The strong hygroscopic nature of DMSO is problematic when contact to humidity cannot be avoided completely, e.g. when analyzing network formation by rheology in situ, since the slightly poor solvent quality of DMSO is continuously reduced with increasing water uptake of DMSO.

The results show that the conversion of the end groups is comparable or somewhat below (for low concentrations) to the data of our previous work [10]. The different philicity of the stars compared to Ref. [10] appears to additionally impact the synthesis in addition to the impact of the aromatic terminal and linker groups. The rheological investigations show a two-stage increase in viscosity during the synthesis, while solutions of the stars with only the 2-(4-nitrophenyl)-benzoxazinone group do not develop associations that are stable on the time scale of the experiment. Thus, the extension of the PCL block via the cross-linking reaction contributes significantly to the assumed associations of the 2-(4-nitrophenyl)-benzoxazinone groups. This contribution was lacking for the networks of Ref. [10] due to a different solvent and different architecture of the stars. However, for both sets of networks, an unexpectedly high apparent content of double links is determined by MQ NMR. In this regard, we cannot discriminate whether this high fraction of double links refers to true double links or just apparent double links via associations and to which extent the amount of true double links is enhanced by associations during cross-linking process. Associations are being reduced with decreasing concentration, i.e. during swelling. Therefore, associations play a lesser role at equilibrium swelling. On the contrary, associations enhance the modulus in the preparation state. Therefore, it is not necessarily a contradiction to observe a similar equilibrium degree of swelling for networks that develop a higher modulus (on the time scale of the rheology) at preparation conditions, since the extra contribution of the associations to modulus is largely reduced at the low concentrations at swelling equilibrium.

CRediT authorship contribution statement

Carolin Bunk: Writing – original draft, Investigation. **Nora Fribiczer:** Investigation, Formal analysis. **Löser Lucas:** Investigation, Formal analysis. **Martin Geisler:** Methodology, Investigation. **Voit Brigitte:** Writing – review & editing, Validation, Supervision. **Sebastian Seiffert:** Writing – review & editing, Supervision, Funding acquisition. **Kay Saalwächter:** Supervision, Methodology, Funding acquisition. **Michael Lang:** Writing – review & editing, Methodology, Funding acquisition, Conceptualization. **Frank Böhme:** Writing – review & editing, Project administration, Funding acquisition, Conceptualization.

Declaration of competing interest

The authors declare that they have no known competing financial interests or personal relationships that could have appeared to influence the work reported in this paper.

Data availability

Data will be made available on request.

Acknowledgements

This work was supported by the German Research Foundation (DFG) and carried out as part of the Research Unit FOR-2811, grant 397384169, and the individual grants 423514254, 423478088, 423435302, 423373052. Carolin Bunk thanks Ronja Bodesheimer, Li Chen and Kerstin Rieβ for performing the syntheses. The Authors thank Dr. Hartmut Komber, Andreas Korwitz and Lisa Ehrlich kindly for recording all HR NMR spectra.

Appendix A. Supplementary data

Supplementary data to this article can be found online at https://doi.org/10.1016/j.polymer.2024.127149.

References

[1] G. Erdodi, J.P. Kennedy, Prog. Polym. Sci. 31 (2006) 1–18.
[2] Z. Mutlu, S. Shams Es-haghi, M. Cakmak, Adv. Healthcare Mater. 8 (2019) 1801390.
[3] N. Hampu, M.A. Hillmyer, ACS Macro Lett. 9 (2020) 382–388.
[4] F.S. Bates, G.H. Fredrickson, Annu. Rev. Phys. Chem. 41 (1990) 525–557.
[5] D.G. Tsalikis, M. Ciobanu, C.S. Patrickios, Y. Higuchi, Macromolecules 56 (2023) 9299–9311.
[6] L.S. Shagolsem, T. Kreer, A. Galuschko, J.-U. Sommer, J. Chem. Phys. 145 (2016).
[7] K.A. Koppi, M. Tirrell, F.S. Bates, K. Almdal, R.H. Colby, J. Phys. II France 2 (1992) 1941–1959.
[8] S. Panyukov, M. Rubinstein, Macromolecules 29 (1996) 8220–8230.
[9] N. Hampu, M.A. Hillmyer, Macromolecules 53 (2020) 7691–7704.
[10] C. Bunk, L. Löser, N. Fribiczer, H. Komber, L. Jakisch, R. Scholz, B. Voit, S. Seiffert, K. Saalwächter, M. Lang, F. Böhme, Macromolecules 55 (2022) 6573–6589.
[11] L. Jakisch, M. Garaleh, M. Schäfer, A. Mordvinkin, K. Saalwächter, F. Böhme, Macromol. Chem. Phys. 219 (2018) 1700327.
[12] C. Bunk, H. Komber, M. Lang, N. Fribiczer, M. Geisler, P. Formanek, L. Jakisch, S. Seiffert, B. Voit, F. Böhme, Polym. Chem. 14 (2023) 1965–1977.
[13] M. Lang, K. Schwenke, J.U. Sommer, Macromolecules 45 (2012) 4886–4895.
[14] K. Schwenke, M. Lang, J.U. Sommer, Macromolecules 44 (2011) 9464–9472.
[15] M. Lang, R. Scholz, L. Löser, C. Bunk, N. Fribiczer, S. Seiffert, F. Böhme, K. Saalwächter, Macromolecules 55 (2022) 5997–6014.
[16] F. Lange, K. Schwenke, M. Kurakazu, Y. Akagi, U.I. Chung, M. Lang, J.U. Sommer, T. Sakai, K. Saalwachter, Macromolecules 44 (2011) 9666–9674.
[17] K. Hagmann, C. Bunk, F. Böhme, R. von Klitzing, Polymers 14 (2022) 2555.
[18] L. Löser, C. Bunk, R. Scholz, M. Lang, F. Böhme, K. Saalwächter, Submitted to Macromolecules, 2023.
[19] N. Fribiczer, K. Hagmann, C. Bunk, F. Böhme, R. von Klitzing, S. Seiffert, submitted to Macromol. Chem. Phys. 225 (2024) 2300389.
[20] C. Lu, S.-r. Guo, Y. Zhang, M. Yin, Polym. Int. 55 (2006) 694–700.
[21] C. Lu, L. Liu, S.-R. Guo, Y. Zhang, Z. Li, J. Gu, Eur. Polym. J. 43 (2007) 1857–1865.
[22] S.J. Buwalda, B. Nottelet, J. Coudane, Polym. Degrad. Stabil. 137 (2017) 173–183.
[23] H.J. Lim, H. Lee, K.H. Kim, J. Huh, C.-H. Ahn, J.W. Kim, Colloid Polym. Sci. 291 (2013) 1817–1827.
[24] Y.K. Choi, Y.H. Bae, S.W. Kim, Macromolecules 31 (1998) 8766–8774.
[25] T.P. Lodge, B. Pudil, K.J. Hanley, Macromolecules 35 (2002) 4707–4717.
[26] K. Mortensen, M. Annaka, ACS Macro Lett. 5 (2016) 224–228.
[27] K. Mortensen, M. Annaka, ACS Macro Lett. 7 (2018) 1438–1442.
[28] D.E. Apostolides, C.S. Patrickios, M. Simon, M. Gradzielski, A. Blanazs, C. Mussault, A. Marcellan, N. Alexander, C. Wesdemiotis, Polym. Chem. 14 (2023) 201–211.
[29] L. Löser, C. Bunk, R. Scholz, M. Lang, F. Böhme, K. Saalwächter, Macromolecules57 (2024) 940–954.
[30] C. Saldías, Á. Leiva, S. Bonardd, C. Quezada, S. Saldías, M. Pino, D. Radic, React. Funct. Polym. 96 (2015) 78–88.
[31] B. Neises, W. Steglich, Angew. Chem., Int. Ed. Engl. 17 (1978) 522–524.
[32] G. Höfle, W. Steglich, H. Vorbrüggen, Angew. Chem., Int. Ed. Engl. 17 (1978) 569–583.
[33] W. Burchard, in: Branched Polymers II, Springer, 1999, pp. 113–194.
[34] v.G. Schulz, F. Blaschke, J. Prakt, Chem 158 (1941) 130–135.
[35] J. Baum, M. Munowitz, A.N. Garroway, A. Pines, J. Chem. Phys. 83 (1985) 2015–2025.
[36] M. Ahmadi, L. Löser, K. Fischer, K. Saalwächter, S. Seiffert, Macromol. Chem. Phys. 221 (2020) 1900400.
[37] R.O.M. Newville, A. Nelson, A. Ingargiola, T. Stensitzki, D. Allan, A. Fox, F. Carter, M. Ray Osborn, D.P. lneuhaus, S. Weigand, G.C. Deil, Allan L. Mark, R. Hansen, G. Pasquevich, J. (2021), https://doi.org/10.5281/zenodo.5570790.
[38] P. Nicolella, M.F. Koziol, L. Löser, K. Saalwächter, M. Ahmadi, S. Seiffert, Soft Matter 18 (2022) 1071–1081.
[39] X. Lou, B.F.M. de Waal, J.L.J. van Dongen, J.A.J.M. Vekemans, E.W. Meijer, J. Mass Spectrom. 45 (2010) 1195–1202.
[40] A. Alanazi, S. Alshehri, M. Altamimi, F. Shakeel, J. Mol. Liq. 299 (2020) 112211.
[41] C.M. Hansen, Hansen Solubility Parameters: a User's Handbook, 2 edn., CRC Press, Boca Raton, 2007.
[42] X. Qin, D. Wu, J. Therm. Anal. Calorim. 107 (2012) 1007–1013.
[43] R. Ellson, R. Stearns, M. Mutz, C. Brown, B. Browning, D. Harris, S. Qureshi, J. Shieh, D. Wold, Comb. Chem. High Throughput Screen. 8 (2005) 489–498.
[44] M. Şimşek, J. Mater. Res. 35 (2020) 332–342.
[45] C. Ramos, G.-M. Lanno, I. Laidmäe, A. Meos, R. Härmas, K. Kogermann, Int. J. Polym. Mater. 70 (2021) 880–892.
[46] S. César, L. Ángel, B. Sebastián, Q. Caterina, S. Soledad, P. Maximiliano, R. Deodato, React. Funct. Polym. 96 (2015) 78–88.
[47] T. Alfrey, A. Bartovics, H. Mark, J. Am. Chem. Soc. 64 (1942) 1557–1560.
[48] M. Rubinstein, R.H. Colby, Polymer Physics, Oxford university press, New York, 2003.
[49] M. Kurakazu, T. Katashima, M. Chijiishi, K. Nishi, Y. Akagi, T. Matsunaga, M. Shibayama, U.-i. Chung, T. Sakai, Macromolecules 43 (2010) 3935–3940.
[50] M. Lang, Macromolecules 46 (2013) 9782–9797.
[51] M. Lang, ACS Macro Lett. 7 (2018) 536–539.
[52] J. Bastide, C. Picot, S. Candau, J. Macromol. Sci. Phys. 19 (1981) 13–34.
[53] P.J. Flory, Principles of Polymer Chemistry, Cornell university press, 1953.
[54] M.A. Woodruff, D.W. Hutmacher, Prog. Polym. Sci. 35 (2010) 1217–1256.
[55] A.N. Semenov, M. Rubinstein, Macromolecules 31 (1998) 1373–1385.
[56] K.S. Kumar, M. Lang, Macromolecules 56 (2023) 7166–7183.
[57] K. Rajagopal, A. Mahmud, D.A. Christian, J.D. Pajerowski, A.E. Brown, S. M. Loverde, D.E. Discher, Macromolecules 43 (2010) 9736–9746.
[58] K. Saalwächter, in: G.A. Webb (Ed.), Modern Magnetic Resonance, Springer International Publishing, Cham, 2017, pp. 1–28.